JOURNAL OF NATURAL PRODUCTS

Article

pubs.acs.org/jnp

Oxasqualenoids from *Laurencia viridis*: Combined Spectroscopic–Computational Analysis and Antifouling Potential

Francisco Cen-Pacheco,[†,‡] Adrián J. Santiago-Benítez,[†,§] Celina García,[†,§] Sergio J. Álvarez-Méndez,[†,§] Alberto J. Martín-Rodríguez,[†,⊥] Manuel Norte,[†,§] Victor S. Martín,[†,§] José A. Gavín,[†,§] José J. Fernández,*[,†,§] and Antonio Hernández Daranas*[,†,∥]

[†]Institute of Bio-Organic Chemistry "Antonio González", Center for Biomedical Research of the Canary Islands (CIBICAN), [§]Department of Organic Chemistry, and [∥]Department of Chemical Engineering and Pharmaceutical Technology, Faculty of Health Sciences, University of La Laguna, Avenida Astrofísico Francisco Sánchez 2, 38206, Tenerife, Spain

[‡]Faculty of Bioanalysis, Campus-Veracruz, Universidad Veracruzana, 91700, Veracruz, México

[⊥]Oceanic Platform of the Canary Islands (PLOCAN), Carretera de Taliarte s/n, 35214, Telde, Gran Canaria, Spain

Supporting Information

ABSTRACT: The chemical study of the red alga *Laurencia viridis* has led to the isolation of four new polyether triterpenoids: 28-hydroxysaiyacenol B (**2**), saiyacenol C (**3**), 15,16-epoxythyrsiferol A (**4**), and 15,16-epoxythyrsiferol B (**5**). The structures of **2** and **3** were established mainly by NMR data analysis and comparison with the well-known metabolite dehydrothyrsiferol (**1**). However, due to the existence of a nonprotonated carbon within the epoxide functionality, stereochemical assignments in **4** and **5** required an in-depth structural study that included NOESY data, *J*-based configuration analysis, comparison with synthetic models, and DFT calculations. The biological activities of the new metabolites and other related oxasqualenoids were evaluated for the first time against a panel of relevant biofouling marine organisms, and structure–activity conclusions were obtained.

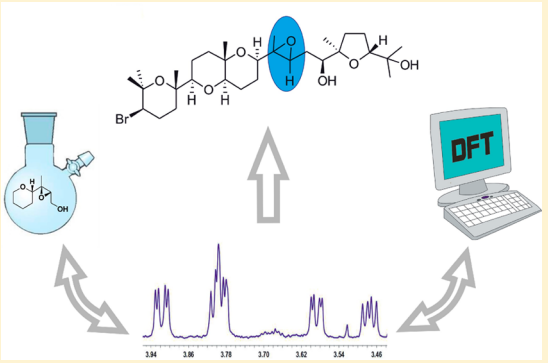

Marine polyethers constitute an important class of bioactive compounds among marine natural products.[1,2] Many have been widely used as research tools to unravel complex biochemical pathways, and some of them have entered clinical trials or are close to that stage, as a result of their attractive pharmacological properties.[3,4] The red alga *Laurencia viridis* produces an amazing variety of these metabolites, with dehydrothyrsiferol (**1**) as a key example, some of which have shown bioactivity as Ser-Thr protein phosphatase 2A inhibitors or integrin antagonists or cytotoxicity.[5,6] This report describes the investigation of *L. viridis* collected from the coastal rocks of the Canary Islands, leading to the isolation of four new metabolites: 28-hydroxysaiyacenol B (**2**), saiyacenol C (**3**), and 15,16-epoxythyrsiferols A and B (**4** and **5**). Their structures were determined on the basis of detailed spectroscopic studies, including a *J*-based configuration approach, comparison with synthetic models, and DFT theoretical calculations. These compounds were evaluated for their antifouling activity toward a panel of organisms composed by marine bacteria, marine-derived fungi, benthic diatoms, and macroalgal zoospores.

RESULTS AND DISCUSSION

Isolation, Structure Determination, and Synthesis of Simplified Models. Specimens of *L. viridis* collected in spring 2013 along the coast of Tenerife (Canary Islands, Spain) were extracted with $CHCl_3$/MeOH (1:1) at room temperature, yielding 83.0 g of a dark green, viscous oil after solvent evaporation. This extract was first separated on a Sephadex LH-20 column using MeOH as the mobile phase, and the enriched polyether fraction was subsequently processed using Lobar LiChroprep-RP18 and Lobar LiChroprep Si-60 columns. The resulting fractions were further purified by HPLC on a μ-Porasil column using *n*-hexane/EtOAc/MeOH, 18:15:5, and *n*-hexane/acetone, 7:3, sequentially to afford four new polyether compounds, 28-hydroxysaiyacenol B (**2**), saiyacenol C (**3**), 15,16-epoxythyrsiferol A (**4**), and 15,16-epoxythyrsiferol B (**5**).

The molecular formula of 28-hydroxysaiyacenol B (**2**), $C_{30}H_{51}BrO_7$, was deduced by HRESIMS, accounting for five unsaturations. This was consistent with its ^{13}C NMR data, where seven methyls, 11 methylenes, six methines, and six nonprotonated carbons bearing oxygen were detected; the absence of sp^2 carbons and carbonyl groups indicates that **2** should be a pentacyclic molecule. Examination of the observed ^{13}C chemical shifts indicated that **2** belongs to the marine polyether triterpene family of compounds typically found in *Laurencia*.[7] Among these metabolites, saiyacenols A (**6**) and B (**7**) showed similar NMR data, although with chemical shift

Received: November 10, 2014

DOI: 10.1021/np5008922
J. Nat. Prod. XXXX, XXX, XXX−XXX

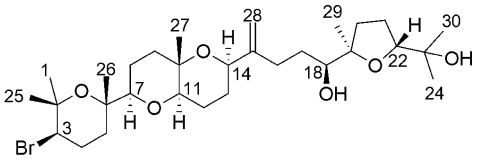

1 Dehydrothyrsiferol

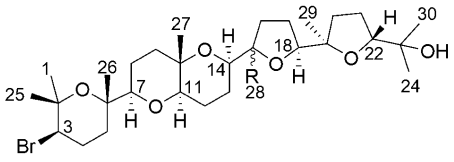

2 28-Hydroxysaiyacenol B; R=CH_2OH; 15S*
6 Saiyacenol A; R=CH_3; 15S*
7 Saiyacenol B; R=CH_3; 15R*
8 28-Hydroxysaiyacenol A; R=CH_2OH; 15R*

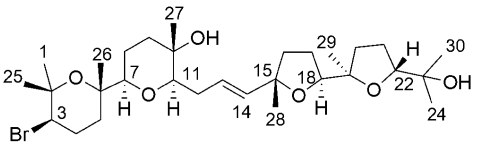

3 Saiyacenol C

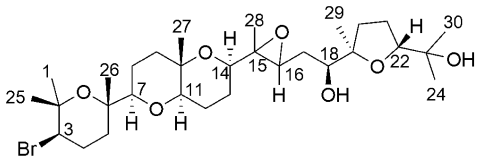

4 Epoxythyrsiferol A; 15S*, 16R*
5 Epoxythyrsiferol B; 15R*, 16S*

differences around the C-15→C-18 region (Table 1).[8] In addition, the molecular formula of **2** indicated the existence of an additional oxygen atom compared to **6** and **7**.

Analysis of COSY and HSQC spectra disclosed the existence of five $^1H-^1H$ spin systems with very similar chemical shifts to those of **6** and **7**: I [H-3→H_2-5]; II [H-7→H_2-9]; III [H-11→H-14]; IV [H_2-16→H-18]; and V [H_2-20→H-22] (Figure 1). Finally, both H_2-28 showed an indistinguishable chemical shift at δ_H 3.55 clearly suggesting the presence of an additional primary alcohol at C-28. Long-range $^1H-^{13}C$ connectivities extracted from the HMBC experimental data allowed linking the previous $^1H-^1H$ spin systems. Particularly important were the long-range correlations observed from the methyl groups, CH_3-1/CH_3-25 to C-2 and C-3; CH_3-26 to C-5, C-6, and C-7; CH_3-27 to C-9, C-10, and C-11; H_3-29 to C-18, C-19, and C-20; and finally CH_3-24/CH_3-30 to C-22 and C-23, that secured the assignments. Moreover, HMBC correlations between CH_2-28 and C-14, C-15, and C-16 supported the previous conclusions and allowed the determination of the planar structure of **2** as shown in Figure 1.

The stereostructure of **2** was established by examination of the ROESY experiment together with a comparison of its ^1H and ^{13}C chemical shift values with those available for other related molecules. Thus, the relative configuration of the three oxane rings and the C-19→C-22 oxolane ring was defined as identical to those of **6** and **7**. Key dipolar correlations were observed between H_3-1/H-3, H_3-25/H_3-26, H-7/H-11, H-11/H-14, H-8β/H_3-27, and H-12β/H_3-27 (Figure 1). A *cis*-configuration was predicted for the oxolane ring at C-15→C-18 after the observation of a clear ROE correlation between H-18 and H_2-28. However, as it was the case for **6** and **7**, assignment of the relative configurations of C-14 and C-15 in **2** was complicated by the fact that these stereocenters are connected by a single bond and C-15 is a nonprotonated carbon, limiting the number of accessible geometrical restraints. Therefore, in order to confirm the stereochemical proposal, both C-15 epimers of compound **2** were obtained using a semisynthetic approach starting from a known compound, dehydrothyrisferol (**1**) (Scheme 1).[9] Thus, a solution of **1** (1.5 mg/0.5 mL) in CH_2Cl_2 was stirred at room temperature while adding *m*-chloroperbenzoic acid (MCPBA; 1.5 equiv) to afford a mixture of two C-15 epimers (**2** and **8**), which were separated by HPLC with a μ-Porasil column using a mixture of *n*-hexane/acetone (7:3). The stereostructure of C-15 in **2** was secured as

Table 1. NMR Spectroscopic Data (^1H 600 MHz, ^{13}C 150 MHz, $CDCl_3$) for Compounds 2 and 3

	28-hydroxysaiyacenol B (**2**)		saiyacenol C (**3**)	
C	δ_C, type	δ_H (J in Hz)	δ_C, type	δ_H (J in Hz)
1	31.0, CH_3	1.26, s	31.0, CH_3	1.26, s
2	75.0, C		75.1, C	
3	59.0, CH	3.90, dd (4.2, 12.4)	59.0, CH	3.88, dd (4.5, 12.1)
4	28.2, CH_2	α 2.10, m	28.2, CH_2	α 2.08, m
		β 2.24, m		β 2.24, m
5	37.1, CH_2	α 1.54, m	37.4, CH_2	α 1.53, m
		β 1.81, m		β 1.83, m
6	74.4, C		74.5, C	
7	86.5, CH	3.06, dd (2.1, 11.5)	86.3, CH	2.98, dd (1.5,11.0)
8	23.0, CH_2	β 1.44, m	23.3, CH_2	β 1.40, m
		α 1.74, m		α 1.75, m
9	38.6, CH_2	α 1.56, m	39.8, CH_2	α 1.52, m
		β 1.74, m		β 1.8, m
10	72.0, C		70.2, C	
11	76.2, CH	3.62, dd (7.0, 11.5)	84.4, CH	3.09, dd (2.8, 9.9)
12	21.1, CH_2	β 1.50, m	32.0, CH_2	β 2.01, m
		α 1.92, m		α 2.32, m
13	20.8, CH_2	α 1.70, m	124.7, CH	5.64, ddd (6.1, 7.8,16.0)
		β 1.92, m		
14	73.7, CH	4.10, dd (2.0, 13.0)	137.3, CH	5.52, dd (16.0)
15	85.1, C		82.8, C	
16	27.8, CH_2	1.74, m	37.7, CH_2	1.66, m
		1.96, m		
17	27.6, CH_2	1.59, m	27.3, CH_2	1.78, m
		1.88, m		1.85, m
18	85.0, CH	3.85, dd (5.6, 9.5)	84.6, CH	3.89, dd (4.5/12.0)
19	84.0, C		84.7, C	
20	34.5, CH_2	1.64, m	35.4, CH_2	1.72, m
		2.12, m		1.95, m
21	26.2, CH_2	1.81, m	26.6, CH_2	1.83, m
		1.86, m		
22	87.2, CH	3.74, dd (5.8, 9.6)	87.0, CH	3.77, dd (6.3/8.9)
23	70.4, C		70.7, C	
24	24.1, CH_3	1.12, s	24.1, CH_3	1.12, s
25	23.7, CH_3	1.40, s	23.5, CH_3	1.40, s
26	20.0, CH_3	1.20, s	20.2, CH_3	1.19, s
27	21.5, CH_3	1.19, s	20.4, CH_3	1.15, s
28	67.6, CH_2	3.55, bs	27.2, CH_3	1.28, s
29	24.4, CH_3	1.19, s	23.1, CH_3	1.16, s
30	27.7, CH_3	1.21, s	27.7, CH_3	1.21, s

DOI: 10.1021/np5008922
J. Nat. Prod. XXXX, XXX, XXX−XXX

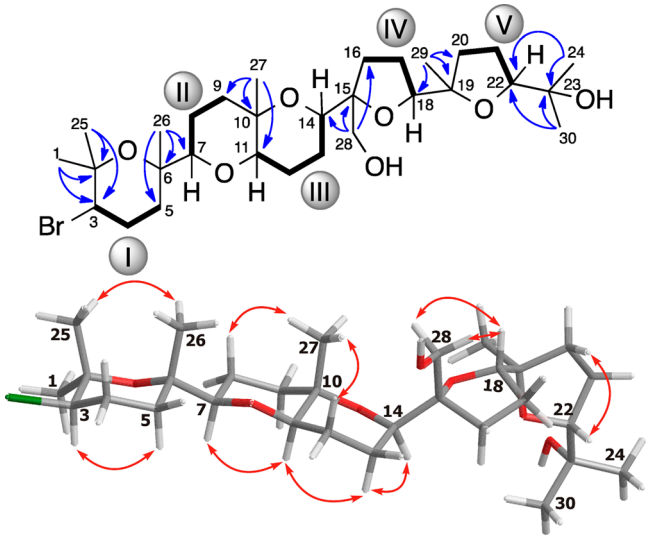

Figure 1. (Top) Selected NMR-derived correlations observed for 28-hydroxysaiyacenol B (**2**). ^{1}H,^{1}H spin systems are numbered from I to V. (Bottom) Key NOE correlations used to determine the relative configuration of **2**.

Scheme 1. Epoxidation of Dehydrothyrsiferol, Yielding Compounds 2 and 8

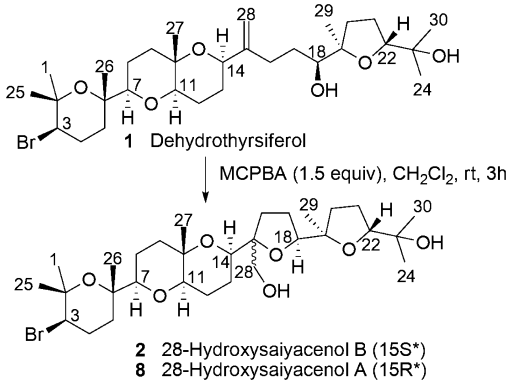

*S** by observation of a ROE between H-18 and H_3-28, leaving **8** as its epimer.

Finally, NMR data of the natural 28-hydroxysaiyacenol B were compared with those of the synthetic compounds to find identity with the 15*S** epimer (**2**). Considering that in **1** the stereochemical relationships of C-18 with all other stereocenters were known, this result sets the relative configuration of **2** as 3*R**, 6*S**, 7*R**, 10*S**, 11*R**, 14*R**, 15*S**, 18*S**, 19*R**, 22*R**.

The molecular formula of saiyacenol C (**3**), $C_{30}H_{51}BrO_6$, was deduced by HRESIMS. This observation was consistent with its ^{13}C NMR spectrum, where eight methyls, nine methylenes, seven methines, and six nonprotonated carbons bearing oxygen carbons were detected. According to these data, five degrees of unsaturation, corresponding to one double bond and four rings, were present in **3** (Table 1). Comparison of the observed ^{1}H and ^{13}C NMR chemical shifts of **3** with those previously reported for saiyacenols A (**6**) and B (**7**) suggested the absence of the characteristic C-7→C-14 dioxabicyclo[4.4.0]decane. Now, two signals at δ_H 5.52 and 5.64 ppm, corresponding to an *E* double bond ($J_{H13—H14}$ = 16.0 Hz), were clearly observed in the NMR spectrum. Five ^{1}H−^{1}H spin systems were easily recognized by analysis of the COSY, TOCSY, and HSQC spectra of **3**. Four ^{1}H−^{1}H spin systems, I [C-3→C-5], II [C-7→C-9], IV [C-16→C-18], and V [C-20→C-22], were analogous to those observed in saiyacenols A and B (**6** and **7**). The remaining ^{1}H−^{1}H spin system, III [C-11→C-14], was conveniently assigned starting from methine H-11 (δ_H 3.09), which is coupled with methylene H_2-12 (δ_H 2.01/2.32), and these protons were coupled, in turn, with H-13 (δ_H 5.64), which was further correlated to methine H-14 (δ_H 5.52). Long-range ^{1}H−^{13}C correlations observed in the HMBC spectra were used to link these ^{1}H−^{1}H spin systems. Thus, methyls CH_3-1/CH_3-25 connected with C-2 and C-3; CH_3-26 with C-5, C-6, and C-7; CH_3-27 with C-9, C-10, and C-11; CH_3-29 with C-18, C-19, and C-20; and CH_3-24/CH_3-30 with C-22 and C-23, confirming that fragments C-1→C-11 and C-19→C-24 are identical to those of saiyacenols A (**6**) and B (**7**). Finally, HMBC correlations between H_3-28 (δ_H 1.28) and C-14 (δ_C 137.3), C-15 (δ_C 82.8), and C-16 (δ_C 37.7) allowed us to determine the planar structure of **3** as shown in Figure 2.

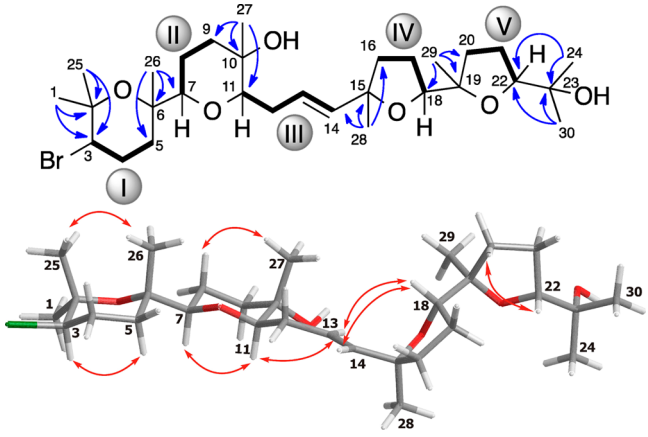

Figure 2. (Top) Selected NMR-derived correlations observed for saiyacenol C (**3**). ^{1}H,^{1}H spin systems are numbered from I to V. (Bottom) Key NOE correlations used to determine the relative configuration of **3**.

Examination of the ROESY experiment allowed us to obtain a number of key correlations (H_3-1/H-3, H_3-25/H_3-26, H-7/H-11, and H-8β/H_3-27) that secured the relative configuration within the two oxane rings present in **3**. Relative configurations within the C-15→C-18 oxolane ring were established by observation of dipolar correlations between the pair of olefinic protons H-13/H-14 and H-18, locating them in the same side of the ring (Figure 2). Finally, the relationship between the configurations of C-18 and C-19 was established comparing the chemical shifts of **3** with those of two molecules sharing the same C-15→C-24 moiety: saiyacenol A (**6**) and a synthetic penta-THF (18*S**,19*R** and 18*R**,19*R**, respectively, Supporting Information).[10] Thus, using the DP4 parameter,[11] the relative configuration 3*R**, 6*S**, 7*R**, 10*S**, 11*R**, 15*S**, 18*S**, 19*R**, and 22 *R** was selected for **3** with a 92.3% probability. This result is in perfect agreement with the fact that a 18*S**, 19*R** relationship has been found for all natural compounds belonging to the thyrsiferol series.[1]

15,16-Epoxythyrsiferol A (**4**) was isolated as an amorphous solid, and its molecular formula was determined as $C_{30}H_{51}BrO_7$ based on HRESIMS measurements. Analysis of its ^{13}C and ^{1}H NMR data indicated the presence of eight methyls, nine methylenes, seven methines, and six nonprotonated carbons

DOI: 10.1021/np5008922
J. Nat. Prod. XXXX, XXX, XXX−XXX

bearing oxygen (Table 2). The absence of olefinic carbons in this molecule suggested the presence of five oxygenated rings.

Table 2. NMR Spectroscopic Data (^{1}H 600 MHz, ^{13}C 150 MHz, $CDCl_3$) for Compounds 4 and 5

	15,16-epoxythyrsiferol A (4)		15,16-epoxythyrsiferol B (5)	
C	δ_C, type	δ_H (J in Hz)	δ_C, type	δ_H (J in Hz)
1	31.0, CH_3	1.27, s	31.2, CH_3	1.27, s
2	75.0, C		74.9, C	
3	59.0, CH	3.89, dd (4.1, 12.4)	58.8, CH	3.89, dd (4.0, 12.4)
4	28.2, CH_2	α 2.10, m	28.2, CH_2	α 2.10, m
		β 2.24, m		β 2.24, m
5	37.1, CH_2	α 1.53, m	37.1, CH_2	α 1.53, m
		β 1.80, m		β 1.80, m
6	74.4, C		74.3, C	
7	86.5, CH	3.04, dd (2.6, 11.5)	86.6, CH	3.04, dd (2.6, 11.5)
8	23.0, CH_2	β 1.45, m	23.0, CH_2	β 1.45, m
		α 1.74, m		α 1.74, m
9	38.6, CH_2	α 1.53, m	38.6, CH_2	α 1.53, m
		β 1.79, m		β 1.79, m
10	72.0, C		72.0, C	
11	77.1, CH	3.44, dd (6.5, 11.1)	77.7, CH	3.38, dd (6.5, 11.1)
12	21.3, CH_2	β 1.54, m	21.3, CH_2	β 1.54, m
		α 1.83, m		α 1.83, m
13	22.1, CH_2	α 1.79, m	22.3, CH_2	α 1.70, m
		β 1.91, m		β 1.83, m
14	74.2, CH	3.56, dd (3.6, 10.7)	74.6, CH	3.66, dd (3.6, 10.7)
15	60.9, C		60.9, C	
16	61.6, CH	3.08, dd (4.9, 7.3)	58.7, CH	3.12, dd (4.9, 7.3)
17	30.6, CH_2	1.54, ddd (7.3, 10.5, 14.2)	31.1, CH_2	1.56, m
		1.88, ddd (2.1, 4.9, 14.2)		2.08, m
18	75.9, CH	3.75, dd (2.1, 10.5)	74.3, CH	3.76, dd (2.1, 10.5)
19	85.4, C		85.8, C	
20	32.6, CH_2	1.64, m	32.6, CH_2	1.64, m
		2.12, m		2.12, m
21	26.5, CH_2	1.86, m	26.5, CH_2	1.86, m
22	87.5, CH	3.77, dd (5.9, 10.0)	87.9, CH	3.77, dd (5.9, 10.0)
23	70.4, C		70.4, C	
24	24.0, CH_3	1.13, s	24.0, CH_3	1.13, s
25	23.6, CH_3	1.40, s	23.6, CH_3	1.40, s
26	20.1, CH_3	1.19, s	20.0, CH_3	1.20, s
27	20.7, CH_3	1.23, s	20.7, CH_3	1.23, s
28	12.4, CH_3	1.27, s	13.6, CH_3	1.30, s
29	23.0, CH_3	1.15, s	23.8, CH_3	1.16, s
30	27.7, CH_3	1.22, s	27.7, CH_3	1.22, s

Analysis of COSY and HSQC spectra allowed us to build five ^{1}H−^{1}H spin systems: I [C-3→C-5], II [C-7→C-9], III [C-11→C-14], IV [C-16→C-18], and V [C-20→C-22]. In this case, spin system IV [C-16→C-18] was different from those of **2** and **3**, as it contains only one methylene (Figure 3). This substructure was conveniently started from methine H-16 (δ_H 3.08), which is coupled with methylene H_2-17 (δ_H 1.54/1.88), and this in turn with H-18 (δ_H 3.75). Next, IV was connected with its neighbor fragments through the HMBC experiment,

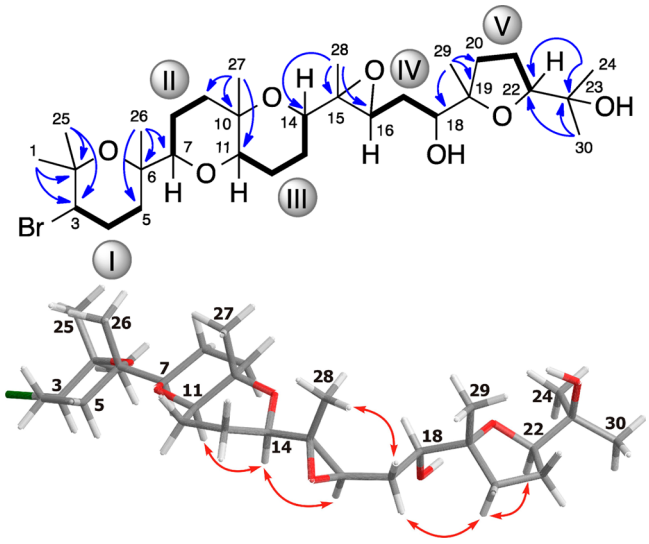

Figure 3. (Top) Selected NMR-derived correlations observed for 15,16-epoxythyrsiferol A (**4**). ^{1}H,^{1}H spin systems are numbered from I to V. (Bottom) Key NOE correlations used to determine the relative configuration of **4**.

where H_3-28 (δ_H 1.27) was correlated with C-14 (δ_C 74.2), C-15 (δ_C 60.9), and C-16 (δ_C 61.6), as well as by the correlations of methyl H_3-29 (δ_H 1.15) with C-18 (δ_C 75.9), C-19 (δ_C 85.4), and C-20 (δ_C 32.6). Other HMBC connectivities confirmed the presence of the bromopyran dioxabicyclo[4.4.0]decane and the terminal oxolane ring. Finally, due to the characteristic chemical shifts of C-15 and C-16, the presence of an epoxide functionality within fragment IV, accounting for the last cyclic system within this molecule, was determined.

The stereostructure of **4** was initially accomplished using dipolar correlations extracted from the NOESY experiment (H_3-1/H-3, H_3-25/H_3-26, H-7/H-11, and H-8β/H_3-27) that allowed us to ensure the relative configuration within the C-1→C-14 moiety of **4** as identical to those identified in **1**, **2**, **6**, **7**, and **8**. Determination of the stereochemical relationship between C-18 and C-19, connected by a single bond, was complicated because C-19 is a nonprotonated carbon, thus reducing the number of coupling constants available for measurement.[12] Nevertheless, the observed values of $^2J_{C19-H18}$ = 2.5 Hz, $^3J_{C20-H18}$ = 3.5 Hz, and $^3J_{C29-H18}$ = 2.7 Hz, together with the NOE between H-17α (δ_H 1.54) and H-20α (δ_H 2.12), supported the 18*S**, 19*R** relative configuration (Figure 4), equal to that observed in dehydrothyrsiferol (**1**). In addition, ^{1}H and ^{13}C chemical shifts and coupling constants along the C-18→C-24 moiety of **4** exhibited very good correspondence with those of **1** (Table S6, Supporting Information), reinforcing the previous conclusion. The relative configurations of C-16 and C-18 were related using a *J*-based configurational approach, measuring coupling constants ($^3J_{H,H}$, $^2J_{C,H}$, and $^3J_{C,H}$) that can be used in cyclic or linear systems.[13,14] The analysis was conveniently started from the C-18→C-17 bond, where the observed values for $^3J_{H18-H17b}$ = 10.5 Hz and $^3J_{H18-H17a}$ = 2.1 Hz suggested an *anti*-conformation between H-18 (δ_H 3.75) and H-17b (δ_H 1.54) and a *gauche*-relationship for H-18 and H-17a (δ_H 1.88). Once the positions of both H-17 hydrogens were identified, we proceeded with the C-16→C-17 bond; however it has to be noted that H-16 is attached to one of the epoxy-carbons, so the geometry along this bond is characteristic of such functionality. Thus, the observed values of $^3J_{H17a-H16}$ =

DOI: 10.1021/np5008922
J. Nat. Prod. XXXX, XXX, XXX−XXX

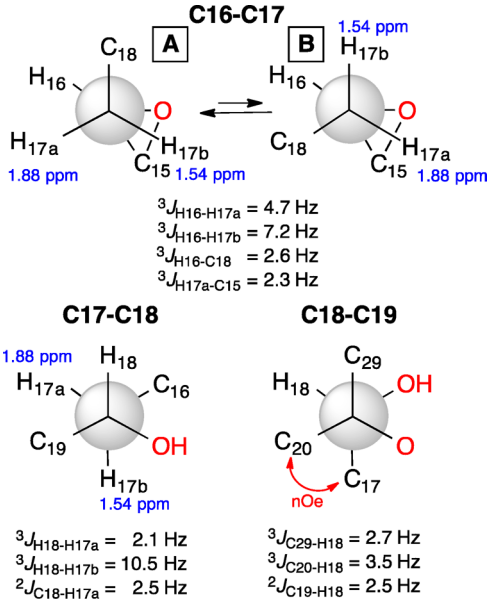

Figure 4. Configurational analysis of fragment C-16→C-19 in 15,16-epoxythyrsiferol A.

4.7 Hz, $^3J_{H17b-H16}$ = 7.2 Hz, $^3J_{C15-H17a}$ = 2.3 Hz, and $^3J_{C18-H16}$ = 2.6 Hz imply a *threo*-configuration between H-16 and H-17a that can be explained by a conformational equilibrium, as shown in Figure 4.[10]

Still, the relative configurations of C-16→C-24 had to be associated with those of C-1→C-14 through the epoxide functionality. Fortunately a very similar metabolite, 15,16-epoxythyrsiferol B (**5**), that was also isolated showed the same molecular formula observed for **4**, $C_{30}H_{51}BrO_7$, as deduced by HRESIMS. In addition, comparison of their ^{1}H and ^{13}C NMR chemical shifts together with an analysis of their 2D NMR data allowed us to establish an identical planar structure for both compounds. Nevertheless, ^{1}H and ^{13}C NMR chemical shifts of the C-15→C-18 moiety, including methyl C-28, showed subtle discrepancies. Therefore, it was concluded that these differences were due to different configurations at C-15 and/or C-16. Next, a *trans*-configuration for the new epoxides (**4** and **5**) was determined by evaluation of the NOESY experiment. Thus, the observation of strong dipolar correlations between H-16 and H-14 and H-18 as well as between H_3-28 and H_2-17 was very informative. Further support for this conclusion was obtained from long-range heteronuclear coupling constants. Thus,

Scheme 2. Synthesis of Model Compounds 14−17

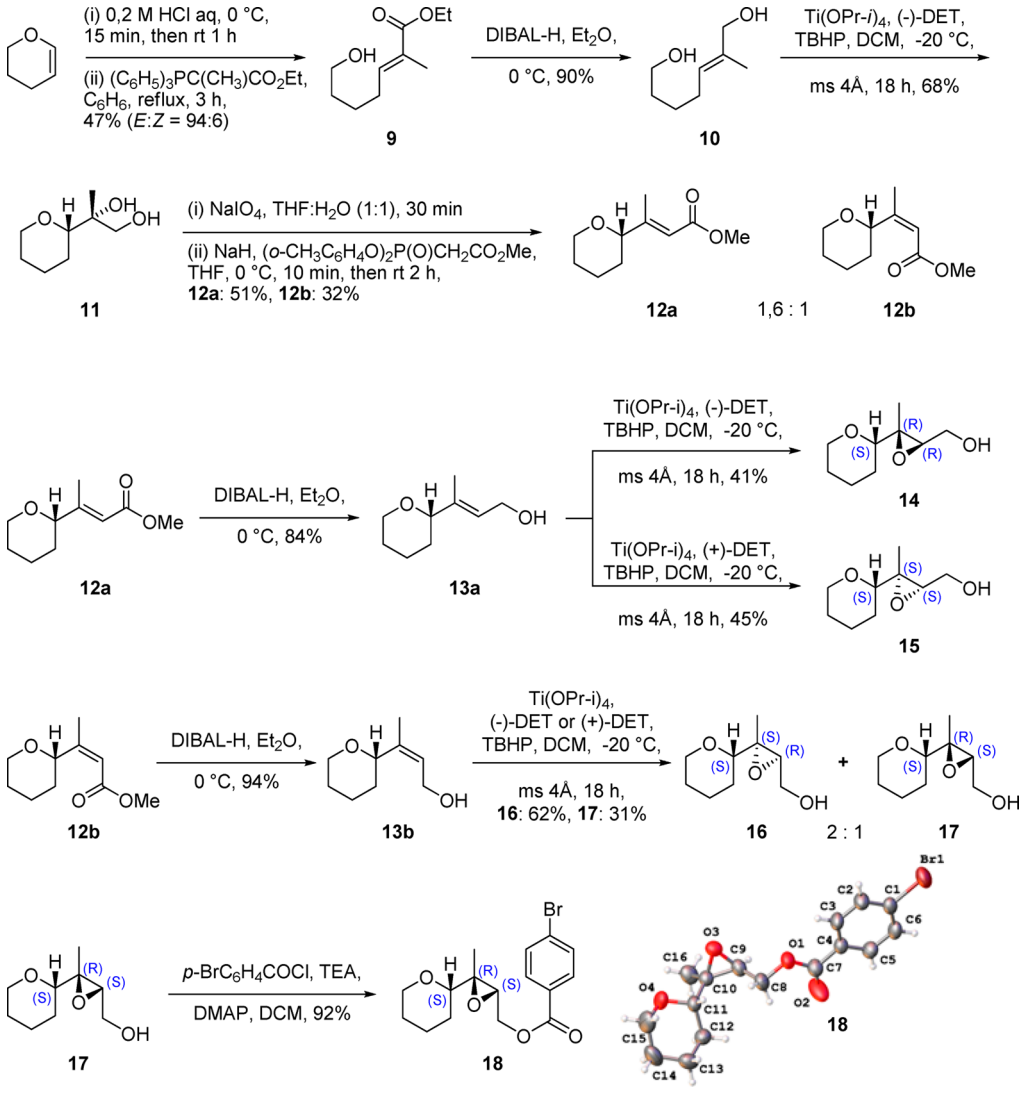

DOI: 10.1021/np5008922
J. Nat. Prod. XXXX, XXX, XXX−XXX

$^3J_{C14-H16}$ = 1.9 Hz was measured for 15,16-epoxythyrsiferol A (**4**) using the *J*HMBC experiment.[15] The measured dihedral angle for a *trans*-configuration is ∼0°, while for a *cis*-configuration it is ∼120°, and in consequence the expected $^3J_{CH}$ value is smaller in *cis*-isomers than in *trans*-isomers. Aliev et al. reported values of <0.5 Hz for the *cis*-isomers and ∼2 Hz for the *trans*-isomers in a similar structural motif, in agreement with the previous observations.[16] Nevertheless, differentiating the two *trans*-isomers was clearly more challenging. Measurement of a full set of $^nJ_{CH}$ was hindered by the fact that C-15 is a nonprotonated carbon and because the carbon chemical shifts for C-15 and C-16 are very similar in **4** ($\Delta\delta$ = 0.7 ppm). Therefore, simplified models of the epoxides were synthesized to address this problem. Thus, a stereocontrolled synthesis of the four possible diastereomers of (3-methyl-3-((*S*)-tetrahydro-2*H*-pyran-2-yl)oxiran-2-yl)methanol was carried out using 3,4-dihydro-2*H*-pyran as starting material. All stereocenters were introduced taking advantage of the asymmetric Katsuki–Sharpless epoxidation (Scheme 2).[17] The hemiacetal obtained by treatment of 3,4-dihydro-2*H*-pyran with aqueous 0.2 M HCl underwent a Wittig-type reaction in order to obtain the hydroxy-*α*,*β*-unsaturated ester **9**.[18] This ester was reduced using DIBAL-H, and the obtained diol **10** underwent a Katsuki–Sharpless epoxidation reaction using (−)-DET as the chiral ligand. After the oxidative cleavage of **11**, the ketone obtained reacted under Ando phosphonate[19] to give a mixture of the two possible *α*,*β*-unsaturated esters in a 1.6:1 ratio, where the *E*-isomer **12a** was the major product. Compounds **12a** and **12b** were separated by chromatography and reduced to allylic alcohols **13a** and **13b**, respectively, precursors required for the subsequent Katsuki–Sharpless epoxidation. Using **13a** as starting material the epoxide **14** was obtained when (−)-DET was used as the chiral ligand, and the epoxide **15** when (+)-DET was the chiral ligand used. A mixture of the epoxides **16** and **17** in a 2:1 ratio, respectively, by treatment of both (−)- and (+)-DET was obtained when **13b** was used as starting material. In order to confirm the absolute configurations of these two epoxides, the *p*-bromobenzoate derivative **18** of the epoxy alcohol **17** was prepared, and its structure confirmed by X-ray crystallography.

A comparison of the NMR chemical shifts extracted from the synthetic models with those of the natural products allowed us to propose the relative configurations of **4** and **5**. Thus, a significant difference was observed in the natural products between $\delta_{C15} - \delta_{C16}$ = 0.7 ppm for **4** and $\delta_{C15} - \delta_{C16}$ = 2.2 ppm for **5**. This pattern was also found for the synthetic diastereoisomers that showed $\Delta\delta$ = 2.8 ppm for **14** and $\Delta\delta$ = 0.1 ppm for **15**. On the basis of these values, a 14*R**, 15*S**, 16*R** relative configuration in 15,16-epoxythyrsiferol A (**4**) and 14*R**, 15*R**, 16*S** for 15,16-epoxythyrsiferol B (**5**) were proposed.

The synthetic approach was complemented using quantum mechanical calculations of NMR chemical shifts, a tool that has been shown to be successful even in highly complex marine natural products.[20,21] Thus, the two possible C-15→C-16 diastereoisomers were built and conformational searches were performed for each using a hybrid MCMM and low-mode sampling and the MMFF94 force field.[22] Next, all conformers within an energy threshold of 10 kJ/mol of the global minimum found were used as input structures for density functional theory (DFT) calculations using the B3LYP functional and the LAVCP**+ basis set to calculate their relative energies and isotropic chemical shieldings.[23,24] It is noteworthy that although the calculations were performed *in vacuo*, they predicted the same equilibrium along the C-16→C-17 bond that was proposed in $CHCl_3$ on the basis of the coupling constant information (providing a 58:42 ratio for rotamers A and B as depicted in Figure 4).[25] Using these data average chemical shifts were calculated for each diastereoisomer. Finally, the computed and the experimental values were compared using the CP3 parameter, which can be applied to the case of assigning a pair of diastereoisomers when one has both experimental data sets.[26] The result was the assignment of the 3*R**, 6*S**, 7*R**, 10*S**, 11*R**, 14*R**, 15*S**, 16*R**, 18*S**, 19*R**, and 22*R** relative configuration for 15,16-epoxythyrsiferol A (**4**) and 3*R**, 6*S**, 7*R**, 10*S**, 11*R**, 14*R**, 15*R**, 16*S**, 18*S**, 19*R**, and 22*R** for 15,16-epoxythyrsiferol B (**5**) with a probability of 99.9% when both ^{1}H and ^{13}C chemical shifts were taken into account.

Antifouling Studies. Compounds **1**–**4**, **7**, and **8** were evaluated for their antifouling activities toward a panel of organisms composed of marine bacteria, marine-derived fungi, benthic diatoms, and macroalgal zoospores.[27] Whereas none of them displayed activity toward the bacterial and fungal strains used (data not shown), meaningful dose-dependent inhibitions were observed in the diatom growth and zoospore germination assays (Table 3). Thus, dehydrothyrsiferol (**1**) and its congeners saiyacenols B (**7**) and C (**3**) prevented *Navicula* cf. *salinicola* and *Cylindrotheca* sp. growth at micromolar concentrations, while both 28-hydroxysaiyacenols B and A (**2** and **8**) also inhibited the germination of *Gayralia oxysperma* spores. On the basis of these results, it seems clear that the 28-hydroxy functionality is essential for the activity of this polyether skeleton. In fact, **2** and **8** exhibited the most potent activities, showing IC_{50} values in the 10–60 μM range for the three diatom strains tested and an MIC value of 25 μM for *G. oxysperma* zoospore germination. However, it seems that the influence of the C-15 configuration on the bioactivity can be neglected, as both epimers showed similar activities. Another observation that reinforces the previous conclusion about the importance of the 28-hydroxy group is the fact that epoxidation at C-15 and C-16 as in 15,16-epoxythyrsiferol A (**4**) leads to a complete loss of bioactivity. This structural hint is further supported by the lack of activity of the synthetic models (**14**–**17**).

Table 3. Activities (μM) Displayed by Tested Natural and Synthetic Compounds[a]

	IC_{50}			MIC
compound	*Phaeodactylum tricornutum*	*Cylindrotheca* sp.	*Navicula* cf. *salinicola*	*Gayralia oxysperma*
1	>100	17.8	23.7	100
2	18.3	11.6	13.7	25
3	>100	17.1	46.7	>100
4	>100	>100	>100	>100
7	67.7	13.0	17.2	n.t.[b]
8	63.3	23.6	18.0	25
14	>100	>100	>100	>100
15	>100	>100	>100	>100
16	>100	>100	>100	>100
17	>100	>100	>100	>100

[a]IC_{50} values were calculated from three experimental replicates. [b]n.t. = not tested.

DOI: 10.1021/np5008922
J. Nat. Prod. XXXX, XXX, XXX–XXX

CONCLUSIONS

Four new oxasqualenoids (**2**–**5**) were isolated from the red alga *L. viridis*. Their relative configurations were determined by a combined experimental–computational analysis. The existence of two diastereomeric epoxides (**4** and **5**) comprising a nonprotonated carbon complicated the determination of their configurations, making necessary the synthesis of simplified models. The approach used combined the analysis of NOE correlations, homo- and heteronuclear *J* couplings, and chemical shift comparisons with synthetic and computational models. The three different NMR approaches were in agreement with the proposed structures. The methodological approach and the conclusions obtained from the structural study can be of general use for similar functionalities existing in other molecules. Although different bioactivities have been reported for oxasqualenoids, this is the first report on their antifouling activity. Ten compounds (**1**–**4**, **7**, **8**, **14**–**17**) were tested against a panel of biofouling species including marine bacteria and fungi, benthic diatoms, and macroalgal zoospores to get a broad overview of their potential effects. Whereas none of them displayed activity toward the bacterial and fungal strains used, this was not the case in diatom growth and zoospore germination assays (Table 3). On the basis of the results obtained it was concluded that a 28-hydroxy functionality improves the activity of this molecular backbone. On the other hand, an epoxide functional group neighboring C-28 as in 15,16-epoxytirsiferol A (**4**) leads to a complete loss of bioactivity. Given the specific activity of these naturally occurring oxasqualenoieds, particularly the 28-hydroxy derivatives, toward both micro- and macroalgal colonizers at micromolar concentrations, it seems reasonable to postulate a possible ecological role of these secondary metabolites as chemical defenses through a targeted action against algal epibionts.[28]

EXPERIMENTAL SECTION

General Experimental Procedures. All reagents were commercially available and used as received. All solvents were dried and distilled under argon immediately prior to use or stored appropriately. THF and Et_2O were refluxed over sodium and benzophenone. CH_2Cl_2 was distilled from CaH_2. Reactions were monitored by TLC. Flash chromatography was performed with silica gel (230–400 mesh) as the stationary phase and mixtures of *n*-hexane and EtOAc, in different proportions given in each case, as the mobile phase. Melting points were determined on a Büchi B-540 model. Optical rotations were determined on a PerkinElmer 343 polarimeter using a sodium lamp operating at 589 nm. IR spectra were measured on a Bruker IFS 66 spectrometer using a methanolic solution over a NaCl disk or neat. NMR spectra were performed on Bruker Avance 400, 500, or 600 instruments at 300 K, and coupling constants are given in Hz. COSY, 1D/2D TOCSY, HSQC, HMBC, and ROESY experiments were performed using standard pulse sequences. Phase-sensitive ROESY spectra were measured using a mixing time of 500 ms. $^3J_{H,H}$ values were measured from 1D ^{1}H NMR and, when signal overlapping did not permit it, from the TOCSY experiment. J-HMBC pulse sequence was used to measure long-range heteronuclear coupling constants. A *J*-scale factor of 52 was used, and the experiment was optimized for long-range couplings of 2 Hz. Data were processed using Topspin or MestRe software. Mass spectra were recorded on a LCT Premier XE Micromass spectrometer using electrospray ionization. X-ray crystallography was performed using an Oxford Diffraction Supernova System. TLC was performed on AL Si gel. TLC plates were visualized by UV light (254 nm) and by adding a phosphomolybdic acid solution 10 wt % in MeOH or a vanillin solution (6 g of vanillin, 450 mL of EtOH, 40 mL of AcOH, and 30 mL of H_2SO_4).

Biological Material. Specimens of *Laurencia viridis* were collected in April 2013 in the intertidal zone at Paraiso Floral, Tenerife, Canary Islands (28°07′12″ N, 16°46′45″ W). Dried material from the sterile plants, sporophytes, and gametophytes was filed at TFC Phyc 7180 (Herbario de la Universidad de La Laguna, Departamento de Biología Vegetal, Botánica, Tenerife, Spain).

Extraction and Isolation. The specimens of *L. viridis* were extracted with $CHCl_3$/MeOH (1:1) at room temperature (rt), and a dark green, viscous oil was obtained (83.0 g) after concentration under reduced pressure. The extract was first chromatographed using Sephadex LH-20 (7 × 50 cm) using CH_2Cl_2/MeOH (1:1) as the mobile phase. The enriched polyether fraction (53.5 g) collected between 225 and 360 mL was subsequently processed on a silica gel column (7 × 50 cm) using a linear gradient of *n*-hexane/EtOAc (80:20–20:80), and fractions collected between 350 and 500 mL were dried (17.1 g). Next, medium-pressure chromatography was done on Lobar LiChroprep Si-60 using CH_2Cl_2/acetone (8:2) at 1 mL/min, and fractions collected between 80 and 105 min were pooled together (770 mg). Final purification was done on an HPLC with a μ-Porasil column using *n*-hexane/EtOAc/MeOH, 18:15:5, sequentially to afford four new polyethers: 15,16-epoxythyrsiferol A (**4**) (2.5 mg) from fractions collected at 39 min, a 1:4 mixture of **4** and 15,16-epoxythyrsiferol B (**5**) (0.9 mg) from fractions collected at 40 min, 28-hydroxysaiyacenol B (**2**) (2.3 mg) from fractions collected between 54 and 57 min, and saiyacenol C (**3**) (9 mg) from fractions collected between 82 and 88 min.

*28-Hydroxysaiyacenol B (**2**):* amorphous, white solid; $[\alpha]^{25}_D$ +4 (*c* 0.25, CH_2Cl_2); IR ($CHCl_3$) ν_{max} 3385, 2971, 2362, 2334, 1375, 1061 cm^{-1}; ^{1}H NMR ($CDCl_3$, 600 MHz) and ^{13}C NMR ($CDCl_3$, 125 MHz), Table 1; HRESIMS *m*/*z* 627.2634/625.2709 [M + Na]$^+$ (calcd for $C_{30}H_{51}{}^{79}BrNaO_7$, 625.2716).

*Saiyacenol C (**3**):* amorphous, white solid; $[\alpha]^{25}_D$ +20 (*c* 0.15, CH_2Cl_2); IR ($CHCl_3$) ν_{max} 3414, 2973, 2866, 2042, 1458, 1377, 1126 cm^{-1}; ^{1}H NMR ($CDCl_3$, 600 MHz) and ^{13}C NMR ($CDCl_3$, 125 MHz), Table 1; HRESIMS *m*/*z* 611.2823/609.2724 [M + Na]$^+$ (calcd for $C_{30}H_{51}{}^{79}BrNaO_6$, 609.2767).

*15,16-Epoxythyrsiferol A (**4**):* amorphous, white solid; $[\alpha]^{25}_D$ +2 (*c* 0.14, CH_2Cl_2); IR ($CHCl_3$) ν_{max} 3550, 2980, 1470, 1455, 1125 cm^{-1}; ^{1}H NMR ($CDCl_3$, 600 MHz) and ^{13}C NMR ($CDCl_3$, 125 MHz), Table 2; HRESIMS *m*/*z* 627.2694/625.2723 [M + Na]$^+$ (calcd for $C_{30}H_{51}{}^{79}BrNaO_7$, 625.2716).

*Chemical Transformation of Dehydrothyrsiferol (**1**) into 28-Hydroxysaiyacenol B (**2**) and 28-Hydroxysaiyacenol A (**8**).* *m*-Chloroperbenzoic acid (1.5 equiv) was added into a CH_2Cl_2 (0.5 mL) solution containing 1.5 mg of dehydrothyrsiferol (**1**). The resulting mixture was stirred for 3 h at rt. Afterward, the solution was filtered and concentrated to give a solid residue, which was chromatographed using HPLC (μ-Porasil column, *n*-hexane/acetone, 7:3, flow rate 1 mL/min), affording 0.8 mg of 28-hydroxysaiyacenol B (**2**) and 0.6 mg of 28-hydroxysaiyacenol A (**8**).

*28-Hydroxysaiyacenol A (**8**):* amorphous, white solid; $[\alpha]^{25}_D$ +2 (*c* 0.05, CH_2Cl_2); IR ($CHCl_3$) ν_{max} 3385, 2971, 2362, 2334, 1375, and 1061 cm^{-1}; ^{1}H NMR ($CDCl_3$, 600 MHz) and ^{13}C NMR ($CDCl_3$, 125 MHz), Table 2; HRESIMS *m*/*z* 627.2720/625.2711 [M + Na]$^+$ (calcd for $C_{30}H_{51}{}^{79}BrNaO_7$, 625.2716).

Preparation of Synthetic Models. *(*E*)-Ethyl 7-Hydroxy-2-methylhept-2-enoate (**9**).* To 3,4-dihydro-2*H*-pyran (16.6 mL, 178.3 mmol) was added HCl(aq) (38 mL, 0.2 M) at 0 °C. The solution was stirred for 15 min and then stirred at rt for 1 h. The resultant mixture was extracted with CH_2Cl_2. The combined organic layer was washed with saturated aqueous $NaHCO_3$ and brine, dried over $MgSO_4$, filtered, and concentrated under vacuum to afford the crude hemiacetal as a colorless oil.

The hemiacetal (6.6 g, 64.7 mmol) was added to a solution of ethoxycarbonylethylidene triphenylphosphorane (24.2 g, 64.7 mmol) in benzene (100 mL). The mixture was heated under reflux for 3 h, then cooled to rt and concentrated under reduced pressure. Purification by column chromatography afforded the α,β-unsaturated ester **9** (7.88 g, 47% after two steps, *E*:*Z* = 94:6) as a colorless oil. The

DOI: 10.1021/np5008922
J. Nat. Prod. XXXX, XXX, XXX–XXX

observed ^{1}H NMR spectrum was consistent with that previously reported in the literature.[29] R_f: 0.25 (*n*-hexane/EtOAct, 6:4, silica gel).

*(E)-2-Methylhept-2-ene-1,7-diol (**10**).* To a solution of α,β-unsaturated ester **9** (7.88 g, 42.3 mmol) in diethyl ether (423 mL), cooled to 0 °C and under argon atmosphere, was added dropwise DIBAL-H 1 M in cyclohexane (85 mL, 85.0 mmol). The reaction was allowed to warm for 1 h and then was recooled to 0 °C, diluted with diethyl ether (100 mL), treated with distilled H_2O (7.7 mL, 427.8 mmol), and stirred vigorously for 30 min. After that, $MgSO_4$ was added, and 15 min later the mixture was filtered over a Celite pad, washed with diethyl ether, and concentrated. Diol **10** was obtained as a colorless oil after purification by column chromatography (5.49 g, 90%), and the observed ^{1}H NMR spectrum was consistent with that previously reported in the literature.[30] R_f: 0.32 (*n*-hexane/EtOAc, 4:6, silica gel).

*(R)-2-((S)-Tetrahydro-2H-pyran-2-yl)propane-1,2-diol (**11**).* A flask with molecular sieves powder (4 Å) was flamed and then cooled to −20 °C. A solution of diol **10** (1.34 g, 9.29 mmol) in CH_2Cl_2 (93 mL) was added under argon atmosphere, followed by freshly distilled titanium(IV) isopropoxide (3.3 mL, 11.15 mmol) and (−)-diethyl D-tartrate (2.2 mL, 13.01 mmol). After 30 min, *tert*-butyl hydroperoxide solution 5.06 M in isooctane (3.3 mL, 16.72 mmol) was added under an argon atmosphere and then stirred for 18 h. Once the reaction was finished, 15% tartaric acid(aq) (100 mL) was added, and the mixture was vigorously stirred at rt for 15 min. Then the aqueous layer was saturated with NaCl powder and extracted with CH_2Cl_2 (3 × 75 mL), and the combined organic layer was concentrated under vacuum. Purification by column chromatography afforded diol **11** (1.01 g, 68%): white solid; mp 35.8−38.3 °C; ^{1}H NMR (400 MHz, $CDCl_3$) δ 4.00 (1H, d, *J* = 11.0 Hz, H-6′), 3.74 (1H, d, *J* = 11.0 Hz, H-1), 3.27−3.42 (3H, m, H-1, H-2′, H-6′), 2.86−2.99 (2H, m, 2 × OH), 1.84−1.91 (1H, m, H-5′), 1.64 (1H, d, *J* = 12.0 Hz, H-4′), 1.42−1.55 (3H, m, H-3′, H-4′, H-5′), 1.32 (1H, dtd, *J* = 12.0, 12.0, 3.0 Hz, H-3′), 1.06 (3H, s, H-3); ^{13}C NMR (100 MHz, $CDCl_3$) δ 84.6 (CH, C-2′), 73.3 (C, C-2), 69.3 (CH_2, C-6′), 67.7 (CH_2, C-1), 26.2 (CH_2, C-3′ or C-4′), 26.1 (CH_2, C-3′ or C-4′), 23.5 (CH_2, C-5′), 20.4 (CH_3, C-3); EIMS *m*/*z* 129 [M − CH_2OH]$^+$ (80), 111 (35), 85 [M − C(Me)(OH)CH_2OH]$^+$ (100), 57 (59); HRESIMS *m*/*z* 183.0996 [M + Na]$^+$ (calcd for $C_8H_{16}NaO_3$, 183.0997); R_f 0.36 (*n*-hexane/EtOAc, 4:6, silica gel).

*(S,E)-Methyl 3-(Tetrahydro-2H-pyran-2-yl)but-2-enoate (**12a**) and (S,Z)-Methyl 3-(Tetrahydro-2H-pyran-2-yl)but-2-enoate (**12b**).* To a solution of diol **11** (1 g, 6.26 mmol) in a mixture of THF/H_2O, 1:1 (42 mL), was added $NaIO_4$ (2 g, 9.35 mmol), and the mixture was stirred for 30 min. Once the reaction was finished, diethyl ether (20 mL) and H_2O (20 mL) were added, the layers were separated, and the aqueous one was saturated with NaCl powder, extracted with diethyl ether (3 × 20 mL), dried over $MgSO_4$, filtered, and concentrated. NMR analysis of the crude revealed high purity of the yellowish oil (605.8 mg, 76%), so it was immediately employed in the following reaction without further purification.

To a suspension of NaH (109.2 mg, 2.73 mmol) in THF (10 mL) was slowly added, at 0 °C and under an argon atmosphere, a solution of methyl 2-(bis(*o*-tolyloxy)phosphoryl)acetate[17] (977.8 mg, 2.93 mmol) in THF (10 mL). After 10 min, a solution of the crude ketone (250 mg, 1.95 mmol) in THF (10 mL) was added dropwise. The mixture was allowed to warm for 2 h and then was quenched with brine (40 mL). The layers were separated, and the aqueous layer was extracted with diethyl ether (3 × 40 mL). The combined organic layer was dried over $MgSO_4$, filtered, and concentrated in vacuum, and then the crude was purified by column chromatography. A 1.6:1 mixture of the *E*-isomer/*Z*-isomer of the final esters (**12a**: 183.5 mg, 51%; **12b**: 114.7 mg, 32%) was obtained, both as yellowish oils.

12a: yellowish oil; ^{1}H NMR (500 MHz, $CDCl_3$) δ 5.94 (1H, t, *J* = 1.2 Hz, H-2), 4.03−4.07 (1H, m, H-6′), 3.70 (1H, d, *J* = 11.2 Hz, H-2′), 3.68 (3H, s, CO_2Me), 3.47 (1H, td, *J* = 11.5, 2.5 Hz, H-6′), 2.12 (3H, d, *J* = 1.2 Hz, H-4), 1.86−1.92 (1H, m, H-5′), 1.74−1.80 (1H, m, H-3′), 1.49−1.61 (3H, m, 2 × H-4′, H-5′), 1.26−1.35 (1H, m, H-3′); ^{13}C NMR (100 MHz, $CDCl_3$) δ 167.7 (C, C-1), 159.1 (C, C-3), 114.1 (CH, C-2), 81.7 (CH, C-2′), 68.6 (CH_2, C-6′), 51.1 (CH_3, CO_2Me), 31.0 (CH_2, C-3′), 25.9 (CH_2, C-4′), 23.9 (CH_2, C-5′), 15.7 (CH_3, C-4); HRESIMS *m*/*z* 207.0989 [M + Na]$^+$ (calcd for $C_{10}H_{16}NaO_3$, 207.0997); R_f 0.53 (*n*-hexane/EtOAc, 9:1, silica gel).

12b: yellowish oil; ^{1}H NMR (500 MHz, $CDCl_3$) δ 5.60−5.62 (1H, m, H-2), 5.10 (1H, d, *J* = 10.9 Hz, H-2′), 3.96−4.00 (1H, m, H-6′), 3.66 (3H, s, CO_2Me), 3.50 (1H, td, *J* = 11.7, 2.7 Hz, H-6′), 1.91 (3H, d, *J* = 1.2 Hz, H-4), 1.83−1.89 (1H, m, H-4′), 1.65−1.73 (1H, m, H-4′), 1.61−1.64 (1H, m, H-3′), 1.53−1.60 (1H, m, H-5′), 1.48−1.52 (1H, m, H-5′), 1.39−1.47 (1H, m, H-3′); ^{13}C NMR (100 MHz, $CDCl_3$) δ 166.3 (C, C-1), 161.6 (C, C-3), 114.9 (CH, C-2), 77.0 (CH, C-2′), 68.3 (CH_2, C-6′), 51.1 (CH_3, CO_2Me), 30.3 (CH_2, C-3′), 26.0 (CH_2, C-4′), 23.7 (CH2, C-5′), 19.7 (CH_3, C-4); HRESIMS *m*/*z* 207.0989 [M + Na]$^+$ (calcd for $C_{10}H_{16}NaO_3$, 207.0997); R_f 0.65 (*n*-hexane/EtOAc, 9:1, silica gel).

*(S,E)-3-(Tetrahydro-2H-pyran-2-yl)but-2-en-1-ol (**13a**).* Compound **13a** was obtained using the same procedure as for diol **10**, using ester **12a** (134 mg, 0.73 mmol), diethyl ether (7.3 mL), and DIBAL-H 1 M in cyclohexane (1.8 mL, 1.8 mmol). The final product was purified by column chromatography to give the alcohol **13a** (95.8 mg, 84%): yellow oil; $[\alpha]^{25}_D$ −25 (*c* 0.7, $CHCl_3$); ATR-FTIR (neat) ν_{max} 3375, 2935, 2851, 1440, 1264, 1204, 1085, 1038, 1009, 633 cm^{-1}; ^{1}H NMR (400 MHz, $CDCl_3$) δ 5.65 (1H, t, *J* = 6.6 Hz, H-2), 4.19 (2H, d, *J* = 6.7 Hz, H-1), 4.03 (1H, d, *J* = 11.0 Hz, H-6′), 3.65 (1H, d, *J* = 10.7 Hz, H-2′), 3.48 (1H, t, *J* = 11.1 Hz, H-6′), 1.83−1.91 (1H, m, H-5′), 1.68 (3H, s, H-4), 1.42−1.66 (5H, m, 2 × H-3′, 2 × H-4′, 1 × H-5′); ^{13}C NMR (100 MHz, $CDCl_3$) δ 139.9 (C, C-3), 124.3 (CH, C-2), 82.4 (CH, C-2′), 68.8 (CH_2, C-6′), 59.3 (CH_2, C-1), 30.6 (CH_2, C-3′), 26.1 (CH_2, C-4′), 23.8 (CH_2, C-5′), 13.1 (CH_3, C-4); EIMS *m*/*z* 156 [M]$^+$ (1), 141 [M − Me]$^+$ (1), 125 [M + 1 − CH_2OH]$^+$ (100), 69 (31); HRESIMS *m*/*z* 156.1148 (calcd for $C_9H_{16}O_2$ [M + Na]$^+$, 156.1150); R_f 0.12 (*n*-hexane/EtOAc, 7:3, silica gel).

*(S,Z)-3-(Tetrahydro-2H-pyran-2-yl)but-2-en-1-ol (**13b**).* Compound **13b** was obtained using the same procedure as for diol **10**, using ester **12b** (254.4 mg, 1.38 mmol), diethyl ether (14 mL), and DIBAL-H 1 M in cyclohexane (3 mL, 3 mmol, 1 h). The final product was purified by column chromatography to give the alcohol **13b** (202.9 mg, 94%): yellow oil; $[\alpha]^{25}_D$ −12.0 (*c* 1.0, $CHCl_3$); ATR-FTIR (neat) ν_{max} 3371, 2935, 2852, 1440, 1269, 1205, 1085, 1020, 997, 631 cm^{-1}; ^{1}H NMR (500 MHz, $CDCl_3$) δ 5.51 (1H, t, *J* = 7.0 Hz, H-2), 4.08−4.17 (2H, m, H-1), 4.05−4.07 (1H, d, *J* = 10.4 Hz, H-2′), 3.99−4.04 (1H, m, H-6′), 3.47 (1H, t, *J* = 11.5 Hz, H-6′), 1.99 (1H, br s, OH), 1.85−1.90 (1H, m, H-5′), 1.74 (3H, s, H-4), 1.49−1.60 (5H, m, 2 × H-3′, 2 × H-4′, 1 × H-5′); ^{13}C NMR (100 MHz, $CDCl_3$) δ 140.1 (C, C-3), 126.1 (CH, C-2), 77.9 (CH, C2′), 68.8 (CH_2, C-6′), 58.5 (CH_2, C-1), 30.4 (CH2, C-3′), 25.9 (CH_2, C-4′), 23.8 (CH_2, C-5′), 20.1 (CH_3, C-4); EIMS *m*/*z* 156 [M]$^+$ (3), 141 [M − Me]$^+$ (3), 125 [M + 1 − CH_2OH]$^+$ (100), 69 (68); HRESIMS *m*/*z* 179.1044 [M + Na]$^+$ (calcd for $C_9H_{16}NaO_2$, 179.1048); R_f 0.26 (*n*-hexane/EtOAc, 9:1, silica gel).

*((2R,3R)-3-Methyl-3-((S)-tetrahydro-2H-pyran-2-yl)oxiran-2-yl)-methanol (**14**).* Compound **14** was obtained using the same procedure as in the case of diol **11**, using alcohol **13a** (41.7 mg, 0.27 mmol), DCM (2.7 mL), titanium(IV) isopropoxide (0.09 mL, 0.32 mmol), (−)-diethyl D-tartrate (0.06 mL, 0.37 mmol), and *tert*-butyl hydroperoxide solution 5.06 M in isooctane (0.1 mL, 0.48 mmol). The final product was purified by column chromatography to give the epoxy alcohol **14** (18.8 mg, 41%): yellow oil; $[\alpha]^{25}_D$ −7.3 (*c* 0.8, $CHCl_3$); ATR-FTIR (neat) ν_{max} 3424, 2931, 2852, 1441, 1379, 1263, 1205, 1087, 1031, 630 cm^{-1}; ^{1}H NMR (400 MHz, $CDCl_3$) δ 3.97−4.04 (1H, m, H-6′), 3.82 (1H, dd, *J* = 12.1, 4.2 Hz, H-1), 3.70 (1H, dd, *J* = 12.6, 6.5 Hz, H-1), 3.37−3.45 (1H, m, H-6′), 3.13 (1H, t, *J* = 5.4 Hz, H-2), 3.08 (1H, d, *J* = 10.9 Hz, H-2′), 2.13 (1H, br s, OH), 1.83−1.91 (1H, m, H-5′), 1.35−1.61 (5H, m, 2 × H-3′, 2 × H-4′, 1 × H-5′), 1.30 (3H, s, Me); ^{13}C NMR (100 MHz, $CDCl_3$) δ 81.6 (CH, C-2′), 68.8 (CH_2, C-6′), 62.6 (C, C-3), 61.1 (CH_2, C-1), 59.8 (CH, C-2), 27.2 (CH_2, C-3′), 25.9 (CH_2, C-4′), 23.3 (CH_2, C-5′), 13.3 (CH_3, Me); EIMS *m*/*z* 172 [M]$^+$ (1), 141 [M − CH_2OH]$^+$ (9), 112 (19), 85 (100); HRESIMS *m*/*z* 172.1102 [M]$^+$ (calcd for $C_9H_{16}O_3$, 172.1099); R_f 0.16 (*n*-hexane/EtOAc, 6:4, silica gel).

DOI: 10.1021/np5008922
J. Nat. Prod. XXXX, XXX, XXX−XXX

*((2S,3S)-3-Methyl-3-((S)-tetrahydro-2H-pyran-2-yl)oxiran-2-yl)-methanol (**15**).* Compound **15** was obtained using the same procedure as in the case of diol **11**, using alcohol **13a** (41.7 mg, 0.27 mmol), CH_2Cl_2 (2.7 mL), titanium(IV) isopropoxide (0.09 mL, 0.32 mmol), (+)-diethyl D-tartrate (0.06 mL, 0.37 mmol), and *tert*-butyl hydroperoxide solution 5.06 M in isooctane (0.1 mL, 0.48 mmol). The final product was purified by column chromatography to yield the epoxy alcohol **15** (20.5 mg, 45%): yellow oil; $[\alpha]^{25}_D$ −21.9 (*c* 0.9, $CHCl_3$); ATR-FTIR (neat) ν_{max} 3421, 2937, 2854, 1442, 1380, 1263, 1205, 1089, 1042, 630 cm^{-1}; ^1H NMR (400 MHz, $CDCl_3$) δ 3.94−4.01 (1H, m, H-6′), 3.79 (1H, dd, *J* = 12.0, 3.8 Hz, H-1), 3.67 (1H, dd, *J* = 12.0, 6.3 Hz, H-1), 3.35−3.43 (1H, m, H-6′), 3.11 (1H, t, *J* = 5.3 Hz, H-2), 3.01 (1H, d, *J* = 10.1 Hz, H-2′), 2.67 (1H, br s, OH), 1.82−1.89 (1H, m, H-5′), 1.37−1.67 (5H, m, 2 × H-3′, 2 × H-4′, 1 × H-5′), 1.25 (3H, s, Me); ^{13}C NMR (100 MHz, $CDCl_3$) δ 81.3 (CH, C-2′), 68.8 (CH2, C-6′), 61.8 (CH, C-2), 61.7 (C, C-3), 61.0 (CH_2, C-1), 26.8 (CH_2, C-3′), 26.0 (CH_2, C-4′), 23.1 (CH_2, C-5′), 13.0 (CH_3, Me); EIMS *m*/*z* 155 $[M - OH]^+$ (10), 141 $[M - CH_2OH]^+$ (1), 112 (30), 85 (100); HRESIMS *m*/*z* 155.1066 $[M - OH]^+$ (calcd for $C_9H_{15}O_2$, 155.1072); R_f 0.16 (*n*-hexane/EtOAc, 6:4, silica gel).

*((2R,3S)-3-Methyl-3-((S)-tetrahydro-2H-pyran-2-yl)oxiran-2-yl)-methanol (**16**) and ((2S,3R)-3-Methyl-3-((S)-tetrahydro-2H-pyran-2-yl)oxiran-2-yl)methanol (**17**).* A flask with molecular sieves powder (4 Å) was flamed and then cooled to −20 °C. A solution of allylic alcohol **13b** (60 mg, 0.39 mmol) in CH_2Cl_2 (3.9 mL) was added under an argon atmosphere, followed by freshly distilled titanium(IV) isopropoxide (0.15 mL, 0.45 mmol) and (−)-diethyl D-tartrate (0.09 mL, 0.54 mmol). After 30 min, a *tert*-butyl hydroperoxide solution 5.06 M in isooctane (0.15 mL, 0.69 mmol) was added under an argon atmosphere and then stirred for 18 h. Once the reaction was finished, 15% tartaric acid(aq) (9 mL) was added and the mixture was vigorously stirred at rt for 15 min. Then the aqueous layer was extracted with CH_2Cl_2 (3 × 9 mL), and the combined organic layer was concentrated under vacuum. The crude was redissolved in diethyl ether (10 mL), cooled to 0 °C, and treated with previously cooled 15% sodium hydroxide(aq) (10 mL) for 1 min. After that, layers were separated, and the aqueous layer was extracted with diethyl ether (3 × 10 mL). The combined organic layer was dried over $MgSO_4$, filtered, and concentrated under vacuum. After purification by column chromatography, a 2:1 mixture of epoxyalcohol **16** (40.8 mg, 62%) and epoxy alcohol **17** (20.4 mg, 31%) was obtained as an oil. The same yield and proportion were obtained when (+)-diethyl L-tartrate was used instead of (−)-diethyl D-tartrate.

16: yellowish oil; $[\alpha]^{25}_D$ −2.3 (*c* 0.1, $CHCl_3$); $[\alpha]^{25}_D$ −5.2 (*c* 0.7, $(CH_3)_2CO$); ATR-FTIR (neat) ν_{max} 3417, 2938, 2854, 1441, 1380, 1261, 1204, 1086, 1039, 656 cm^{-1}; ^1H NMR (400 MHz, $CDCl_3$) δ 3.99−4.02 (1H, m, H-6′), 3.89 (1H, dd, *J* = 11.4, 4.9 Hz, H-1), 3.66 (1H, dd, *J* = 11.6, 7.3 Hz, H-1), 3.42−3.47 (1H, m, H-6′), 3.20 (1H, d, *J* = 10.7 Hz, H-2′), 3.06 (1H, t, *J* = 6.2 Hz, H-2), 2.48 (1H, br s, OH), 1.88−1.96 (1H, m, H-5′), 1.47−1.74 (5H, m, 2 × H-3′, 2 × H-4′, 1 × H-5′), 1.32 (3H, s, Me); ^{13}C NMR (100 MHz, $CDCl_3$) δ 79.4 (CH, C-2′), 69.1 (CH_2, C-6′), 63.6 (CH, C-2), 61.26 (C, C-3), 61.23 (CH_2, C-1), 27.3 (CH_2, C-3′), 26.0 (CH_2, C-4′), 23.1 (CH_2, C-5′), 18.0 (CH_3, Me); EIMS *m*/*z* 172 $[M]^+$ (1), 141 $[M - CH_2OH]^+$ (82), 112 (24), 85 (100); HRESIMS *m*/*z* 172.1106 $[M - OH]^+$ (calcd for $C_9H_{16}O_3$, 172.1099); R_f 0.39 (*n*-hexane/EtOAc, 6:4 (eluted twice), silica gel).

17: yellowish oil; $[\alpha]^{25}_D$ −34.1 (*c* 0.9, $CHCl_3$); ATR-FTIR (neat) ν_{max} 3425, 2937, 2853, 1441, 1379, 1259, 1205, 1086, 1039, 630 cm^{-1}; ^1H NMR (400 MHz, $CDCl_3$) δ 3.99−4.06 (1H, m, H-6′), 3.78 (2H, d, *J* = 5.6 Hz, H-1), 3.39−3.47 (1H, m, H-6′), 3.25 (1H, t, *J* = 6.2 Hz, H-2′), 2.99 (1H, t, *J* = 5.6 Hz, H-2), 2.13 (1H, br s, OH), 1.83−1.91 (1H, m, H-5′), 1.44−1.62 (5H, m, 1 × H-3′, 2 × H-4′, 2 × H-5′), 1.34 (3H, s, Me); ^{13}C NMR (100 MHz, $CDCl_3$) δ 79.7 (CH, C-2′), 68.8 (CH_2, C-6′), 63.6 (CH, C-2), 63.3 (C, C-3), 60.8 (CH_2, C-1), 28.3 (CH_2, C-3′), 25.9 (CH_2, C-4′), 23.4 (CH_2, C-5′), 18.2 (CH_3, Me); EIMS *m*/*z* 172 $[M]^+$ (1), 141 $[M - CH_2OH]^+$ (100), 112 (16), 85 (84); HRESIMS *m*/*z* 172.1104 $[M]^+$ (calcd for $C_9H_{16}O_3$, 172.1099); R_f 0.29 (*n*-hexane/EtOAc, 6:4 (eluted twice), silica gel).

*((2S,3R)-3-Methyl-3-((S)-tetrahydro-2H-pyran-2-yl)oxiran-2-yl)-methyl 4-Bromobenzoate (**18**).* To a solution of epoxy alcohol **17** (22.9 mg, 0.13 mmol) in dry CH_2Cl_2 (1.3 mL) was added sequentially, at 0 °C and under an argon atmosphere, triethylamine (0.11 mL, 0.78 mmol), 4-bromobenzoyl chloride (116.2 mg, 0.52 mmol), and a catalytic amount of DMAP. The reaction was allowed to warm for 1 h and then was diluted with CH_2Cl_2 (1 mL) and quenched with brine (2 mL). Layers were separated, and the aqueous layer was extracted with CH_2Cl_2 (3 × 2 mL). The combined organic layers was dried over $MgSO_4$, filtered, and concentrated, and the crude was purified by chromatographic column, to yield the *p*-bromobenzoate **18** (43.3 mg, 92%) as a white solid. Pure monoclinic crystals were obtained from crystallization in CH_2Cl_2/*n*-hexane, 9:1: white solid; $[\alpha]^{25}_D$ −29.9 (*c* 1.6, $CHCl_3$); mp 78.3−80.5 °C; ATR-FTIR (neat) ν_{max} 2941, 2855, 1725, 1590, 1264, 1173, 1087, 1007, 865, 753 cm^{-1}; ^1H NMR (400 MHz, $CDCl_3$) δ 7.91 (2H, d, *J* = 8.1 Hz, Ar-H), 7.58 (2H, d, *J* = 8.1 Hz, Ar-H), 4.59 (1H, dd, *J* = 12.2, 3.4 Hz, H-1), 4.33 (1H, dd, *J* = 12.2, 7.2 Hz, H-1), 4.04 (1H, d, *J* = 11.6 Hz, H-6′), 3.44 (1H, t, *J* = 11.2 Hz, H-6′), 3.21 (1H, t, *J* = 6.3 Hz, H-2′), 3.14 (1H, dd, *J* = 7.0, 3.7 Hz, H-2), 1.84−1.92 (1H, m, H-5′), 1.46−1.63 (5H, m, 1 × H-3′, 2 × H-4′, 2 × H-5′), 1.37 (3H, s, Me); ^{13}C NMR (100 MHz, $CDCl_3$) δ 165.8 (C, C-1″), 131.9 (C, 2 × Ar), 131.4 (CH, 2 × Ar), 128.7 (C, Ar), 128.6 (C, Ar), 79.4 (CH, C-2′), 68.7 (CH_2, C-6′), 63.5 (CH, C-2), 62.7 (C, C-3), 60.5 (CH_2, C-1), 28.4 (CH_2, C-3′ or C-4′), 25.8 (CH_2, C-3′ or C-4′), 23.3 (CH_2, C-5′), 17.6 (CH_3, Me); EIMS *m*/*z* 356 $[M]^+$ (1), 155 $[M - OC(O)C_6H_4Br]^+$ (22), 141 $[M - CH_2OC(O)C_6H_4Br]^+$ (9), 85 (100); HRESIMS *m*/*z* 356.0444 $[M]^+$ (calcd for $C_{16}H_{19}BrO_4$, 356.0446); R_f 0.28 (*n*-hexane/EtOAc, 9:1, silica gel).

Computational Methods. Molecular mechanics conformational searches were undertaken using the Macromodel software (version 8.5, Schrödinger Inc.) and the MMFF94 force field.[31] Solvation effects of $CHCl_3$ were simulated using the generalized Born/surface area (GBSA) solvation model. Extended nonbonded cutoff distances (van der Waals cutoff of 8.0 Å and an electrostatic cutoff of 20.0 Å) were used. All local minima within 10 kJ of the global minimum were saved, and the analysis of the results was undertaken using Maestro software. Quantum mechanical calculations were carried out using the Jaguar package (Jaguar; Schrödinger LLC). Single-point energy calculations were performed at the DFT theoretical level in the gas phase. The B3LYP hybrid functional with the LACVP**+ basis set was used. Chemical shifts were calculated from their shielding constants that were first averaged according to their relative Boltzmann populations using a Schrödinger Inc. Python script. Chemical shifts were calculated using the gauge-including atomic orbital (GIAO) method. Proton chemical shifts for each methyl group were averaged due to their conformational freedom.

Diatom Growth Inhibition. Three strains of benthic diatoms, *Phaeodactylum tricornutum*, *Cylindrotheca* sp., and *Navicula* cf. *salinicola* BEA0055, were used to test the effect of the compounds on microalgal growth. Diatoms were cultured at 19 ± 1 °C in Erlenmeyer flaks (250 mL) containing 150 mL of Guillard's F/2 medium and subjected to a photoperiod of 18:6 (L:D). Tests were run in 48-well plates. Inocula were prepared by adjusting the diatom concentration to (1−2) × 10^6 cells/mL using a Neubauer chamber. Test products were dissolved in F/2 medium (500 μL) to which diatom inocula (500 μL) were added. Plates were incubated under the above-mentioned conditions for 5 days, and then chlorophyll-*a* (Chla) was extracted. In order to extract Chla, the plates were centrifuged at 5500 rpm for 15 min. The supernatants were discarded, and 200 μL of DMSO was added to the wells. Then, the content of each well was transferred to a 96-well plate, and the amount of Chla was determined spectrophotometrically.[32] A pathlength correction for the DMSO extracts was applied.[33]

Inhibition of Macroalgal Spore Germination. *Gayralia oxysperma* specimens were collected from the intertidal zone at El Médano beach, Tenerife, Spain. Spores were released in Von Stosch Solution (VSS) by the osmotic method.[34,35] Bioassays were conducted in flat-bottom 96-well plates as described by Chambers et al. with slight modifications.[36] Each well was filled with 50 μL of the appropriate dilution of the products in VSS to which 50 μL of spore inoculum (1.6 × 10^5 spores/mL) was added. Plates were incubated at

DOI: 10.1021/np5008922
J. Nat. Prod. XXXX, XXX, XXX−XXX

19 ± 1 °C for 6 days under a L:D 18:6 photoperiod. After the incubation time, the bottom of each well was inspected for the presence of germinated spores with an inverted microscope. A spore was considered to be germinating if the germ tube was visible. The MIC was recorded as the lowest concentration inhibiting spore germination. Three replicates were prepared for each compound and test concentration. Eight serial 2-fold dilutions, from 100 to 0.7 μM, were assayed for each compound.

■ ASSOCIATED CONTENT

Ⓢ Supporting Information

General experimental procedures, NMR and X-ray crystallographic data, as well as details on computational calculation results. This material is available free of charge via the Internet at http://pubs.acs.org.

■ AUTHOR INFORMATION

Corresponding Authors

*E-mail (J. J. Fernández): jjfercas@ull.es.

*E-mail (A. H. Daranas): adaranas@ull.es.

Notes

The authors declare no competing financial interest.

■ ACKNOWLEDGMENTS

This research was funded by SAF2011-28883-C03-01 and CTQ2011-28417-C02-01/BQU from MINECO and CEI10/00018 from MECyD, Spain, as well as by EU Grants FP7-KBBE-3-245137-MAREX and FP7-REGPOT-2012-CT2012-31637-IMBRAIN. A.J.M.R. holds a 2+2 contract from PLOCAN. S.J.A.-M. thanks the Spanish MECyD for an FPU grant. A.J.S.B. thanks the CajaCanarias Foundation for a grant. The authors are grateful to Dr. M. Sansón, Department of Vegetal Biology, ULL, for her valuable help in the collection and identification of *G. oxysperma* specimens, as well as for insightful comments about algal biology and experimental procedures with zoospores.

■ REFERENCES

(1) Fernández, J. J.; Souto, M. L.; Norte, M. *Nat. Prod. Rep.* **2000**, *17*, 235−246.

(2) Blunt, J. W.; Copp, B. R.; Keyzers, R. A.; Munro, M. H. G.; Prinsep, M. R. *Nat. Prod. Rep.* **2014**, *31*, 160−258.

(3) Cragg, G. M.; Grothaus, P. G.; Newman, D. J. *Chem. Rev.* **2009**, *109*, 3012−3043.

(4) Cragg, G. M.; Grothaus, P. G.; Newman, D. J. *J. Nat. Prod.* **2014**, *77*, 703−723.

(5) Cen-Pacheco, F.; Villa-Pulgarin, J. A.; Mollinedo, F.; Norte, M.; Daranas, A. H.; Fernández, J. J. *Eur. J. Med. Chem.* **2011**, *46*, 3302−3308.

(6) Cen-Pacheco, F.; Villa-Pulgarin, J. A.; Mollinedo, F.; Norte, M.; Fernández, J. J.; Daranas, A. H. *Mar. Drugs* **2011**, *9*, 2220−2235.

(7) Cen-Pacheco, F.; Nordström, L.; Souto, M. L.; Norte, M.; Fernández, J. J.; Daranas, A. H. *Mar. Drugs* **2010**, *8*, 1178−1188.

(8) Cen-Pacheco, F.; Mollinedo, F.; Villa-Pulgarin, J. A.; Norte, M.; Fernández, J. J.; Daranas, A. H. *Tetrahedron* **2012**, *68*, 7275−7279.

(9) González, A. G.; Arteaga, J. M.; Fernández, J. J.; Martín, J. D.; Norte, M.; Ruano, J. Z. *Tetrahedron* **1984**, *40*, 2751−2755.

(10) Caserta, T.; Piccialli, V.; Gomez-Paloma, L.; Bifulco, G. *Tetrahedron* **2005**, *61*, 927−939.

(11) Smith, S. G.; Goodman, J. M. *J. Am. Chem. Soc.* **2010**, *132* (37), 12946−12959.

(12) Bifulco, G.; Dambruoso, P.; Gomez-Paloma, L.; Riccio, R. *Chem. Rev.* **2007**, *107*, 3744−3779.

(13) Matsumori, N.; Kaneno, D.; Murata, M.; Nakamura, H.; Tachibana, K. *J. Org. Chem.* **1999**, *64*, 866−876.

(14) Napolitano, J.; Gavín, J.; García, C.; Norte, M.; Fernández, J. J.; Daranas, A. H. *Chem.—Eur. J.* **2011**, *17*, 6338−6347.

(15) Meissner, A.; Sorensen, O. W. *Magn. Reson. Chem.* **2001**, *39*, 49−52.

(16) Aliev, A. E.; Zakirin, A. M.; Busson, M. J. M.; Fitzmaurice, R. J.; Caddick, S. *J. Org. Chem.* **2012**, *77*, 6290−6295.

(17) Katsuki, T.; Martín, V. S. In *Organic Reactions*; Paquette, L. A., et al., Eds.; Wiley & Sons: New York, 1996; Vol. *48*, pp 1−299.

(18) Hayashi, Y.; Kanayama, J.; Yamaguchi, J.; Shoji, M. *J. Org. Chem.* **2002**, *67*, 9443−9448.

(19) Ando, K. *J. Org. Chem.* **1997**, *62*, 1934−1939.

(20) Cen-Pacheco, F.; Rodríguez, J.; Norte, M.; Fernández, J. J.; Daranas, A. H. *Chem.—Eur. J.* **2013**, *19*, 8525−8532.

(21) Domínguez, H. J.; Crespín, G. D.; Santiago-Benítez, A. J.; Gavín, J. A.; Norte, M.; Fernández, J. J.; Daranas, A. H. *Mar. Drugs* **2014**, *12*, 176−192.

(22) Kolossváry, I.; Guida, W. C. *J. Comput. Chem.* **1999**, *20*, 1671−1684.

(23) Lodewyk, M. W.; Siebert, M. R.; Tantillo, D. R. *Chem. Rev.* **2012**, *112*, 1839−1862.

(24) Rassolov, V. A.; Ratner, M. A.; Pople, J. A.; Redfern, P. C.; Curtiss, L. A. *J. Comput. Chem.* **2001**, *22*, 976−984.

(25) Saielli, G.; Nicolaou, K. C.; Ortiz, A.; Zhang, H.; Bagno, A. *J. Am. Chem. Soc.* **2011**, *133*, 6072−6077.

(26) Smith, S. G.; Goodman, J. M. *J. Org. Chem.* **2009**, *74*, 4597−4607.

(27) Briand, J.-F. *Biofouling* **2009**, *25*, 297−311.

(28) Lane, A. L., Kubanek, J. Secondary Metabolite Defenses against Pathogens and Biofoulers. In *Algal Chemical Ecology*; Amsler, C. D., Ed.; Springer-Verlag: Berlin, 2008; pp 229−243.

(29) Hayashi, Y.; Kanayama, J.; Yamaguchi, J.; Shoji, M. *J. Org. Chem.* **2002**, *67*, 9443−9448.

(30) Orsini, F.; Pelizzoni, F. *J. Org. Chem.* **1980**, *45*, 4726−4727.

(31) *Macromodel*, version 10.0, and *Jaguar*, version 8.0; Schrödinger, LLC: New York, NY, 2013.

(32) Wellburn, A. R. *J. Plant Physiol.* **1994**, *144*, 307−313.

(33) Warren, C. R. *J. Plant Nutr.* **2008**, *31*, 1321−1332.

(34) Fletcher, R. L. *Int. Biodeterior.* **1989**, *25*, 407−422.

(35) Callow, M. E.; Callow, J. A.; Pickett-Heaps, J. D.; Wetherbee, R. *J. Phycol.* **1997**, *33*, 938−947.

(36) Chambers, L. D.; Hellio, C.; Strokes, K. R.; Dennington, S. P.; Goodes, L. R.; Wood, R. J. K.; Walsh, F. C. *Int. Biodeterior. Biodegrad.* **2011**, *65*, 939−946.

DOI: 10.1021/np5008922
J. Nat. Prod. XXXX, XXX, XXX−XXX